inorganics

MDPI

Article

Insights into Molecular Beryllium–Silicon Bonds

Dominik Naglav, Briac Tobey, Kevin Dzialkowski, Georg Jansen, Christoph Wölper and Stephan Schulz *

Faculty of Chemistry and Center for NanoIntegration (CENIDE), University of Duisburg-Essen, DE-45117 Essen, Germany; Dominik.Naglav@uni-due.de (D.N.); briac.tobey@uni-due.de (B.T.); kevin.dzialkowski@stud.uni-due.de (K.D.); georg.jansen@uni-due.de (G.J.); christoph.woelper@uni-due.de (C.W.)

* Correspondence: stephan.schulz@uni-due.de; Tel.: +49-201-183-4635

Academic Editor: Matthias Westerhausen

Received: 23 March 2017; Accepted: 4 April 2017; Published: 10 April 2017

Abstract: We present the synthesis of two silyl beryllium halides HypSiBeX·(thf) (HypSi = $Si(SiMe_3)_3$, X = Cl **2a**, I **4a**) and the molecular structure of **2a** as determined by single crystal X-ray diffraction. Compounds **2a** and **4a** were characterized via multi-nuclear NMR spectroscopy (^{1}H, ^{9}Be, ^{13}C, ^{29}Si), and the bonding situation was further investigated using quantum chemical calculations (with the addition of further halides X = F **1b**, Cl **2b**, Br **3b**, I **4b**). The nature of the beryllium silicon bond in the context of these compounds is highlighted and discussed.

Keywords: beryllium; silicon; main group metal complexes; X-ray diffraction; multi-nuclear NMR spectroscopy; quantum chemical calculations

1. Introduction

The organometallic and coordination chemistry of beryllium has gained attention as several groups, including ours, started to focus their research on this rather unknown and hitherto neglected element [1]. In the last five years, many groundbreaking discoveries, including the first compound with beryllium in the formal oxidation state 0 by the Braunschweig group [2], a beryllium-induced C–N bond activation in an *N*-heterocyclic carbene [3], the structural characterization of the long known $Be(N(SiMe_3)_2)_2$ [4], the synthesis of the first bis(diphenylphosphinimino)methanide and -methanediide beryllium complexes [5], and the synthesis of ether-free beryllium organyls [6], were reported. Even in the field of material chemistry and catalysis, groups around the world started to investigate the unique properties of beryllium compounds [7]. The prejudices and reservations that people might have against beryllium due to its potential risks were discussed and elucidated in our recently reported review [8].

Part of our research focuses on the synthesis of heteroleptic beryllium compounds bearing at least one halide of the RBeX type (R = organic substituent, X = F, Cl, Br, I) and their structural characterization via single crystal X-ray diffraction, multi-nuclear NMR, and quantum mechanical calculations to achieve a deeper understanding of the bonding nature in beryllium compounds [4,9,10]. This led to several publications, which highlight the subtle influences of the substituents on the chemical and electronic properties of the resulting compounds. We extended these studies now to silicon-containing substituents, the heavier congener of carbon. To the best of our knowledge, compounds of the type R'BeX (R = SiR_3, X = F, Cl, Br, I) with a beryllium–silicon bond have to date rarely been studied [11,12]. Our findings are presented in this work to blaze a trail for research on the chemistry of beryllium–silicon compounds and for a deeper understanding of the beryllium–silicon bond.

2. Results and Discussion

2.1. Synthesis

The reaction of $LiSi(SiMe_3)\cdot(thf)_{2.6}$ with BeX_2 (X = Cl, I) in a 1:1 mixture of dry toluene/thf at 60 °C led to the formation of **2a** and **4a** after stirring for 16 h (Scheme 1), which was confirmed by ^{9}Be NMR spectroscopy. All volatiles were removed under reduced pressure, and the residue was dried for 2 h in an oil-pump vacuum. The residue was then dissolved in a small amount of dry toluene and filtrated, and the compounds were crystallized at −28 °C (yield: **2a** 83%, **4a** 87%). **2a** and **4a** were obtained as colorless crystalline solids, which dissolve easily in a number of typical coordinating (Et_2O, THF) and non-coordinating solvents (hexane, cyclohexane, toluene) and were characterized by multi-nuclear NMR spectroscopy (^{1}H, ^{9}Be, ^{13}C, ^{29}Si; Figures S1–S8).

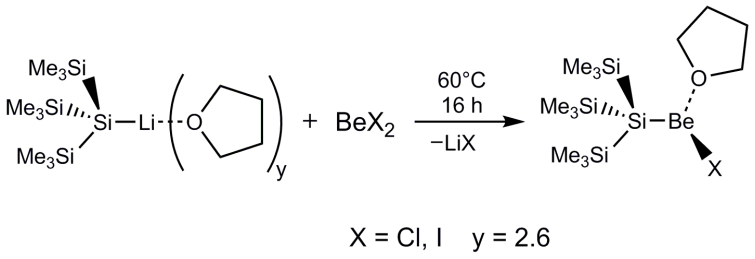

Scheme 1. Synthesis of **2a** and **4a**.

2.2. NMR-Spectroscopy

The ^{9}Be NMR shifts underline that the tetrahedral geometry of the complexes that is found in the solid state is also preserved in solution. The thf molecules are still coordinating with the beryllium. An overview of typical ^{9}Be NMR shifts of several heteroleptic complexes of the general type RBeX depending on the coordination mode is given in Table 1, which also includes ether-coordinated $BeX_2(OEt_2)_2$ (X = Cl, Br), which adopt tetrahedral structures both in solution and in the solid state [13,14], silyl-substituted compounds $CpBeSiR_3$ and $Be[N(SiMe_3)_2]_2$, respectively.

Table 1. Overview of typical ^{9}Be NMR shifts depending on their complex geometry and their respective coordination modes.

Compound	^{9}Be NMR Shifts (δ in ppm)	Solvent	Coordination Mode	Coordination Number	Literature
$(Me_3Si)_3SiBeCl\cdot(thf)$	2.45	thf-d_8	tetrahedral	4	this work
$(Me_3Si)_3SiBeI\cdot(thf)$	−0.92	thf-d_8	tetrahedral	4	this work
$BeCl_2(OEt_2)_2$	2.6	C_6D_6	tetrahedral	4	[13]
$BeBr_2(OEt_2)_2$	3.0	C_6D_6	tetrahedral	4	[13]
$CpBeSiMe_3$	−27.70	C_6D_6	aromatic (η^5)	6	[12]
$CpBe(SiMe_2SiMe_3)$	−27.20	C_6D_6	aromatic (η^5)	6	[12]
TpBeF	4.54	thf-d_8/C_7D_8 3:5	tetrahedral	4	[9]
TpBeCl	4.95	thf-d_8	tetrahedral	4	[9]
TpBeBr	5.15	thf-d_8/C_6D_6 1:3	tetrahedral	4	[9]
TpBeI	4.66	thf-d_8	tetrahedral	4	[9]
$Tp^{tBu}BeCl$	2.7	C_6D_6	tetrahedral	4	[15]
$Tp^{tBu}BeBr$	2.4	C_6D_6	tetrahedral	4	[15]
$Tp^{tBu}BeI$	1.3	C_6D_6	tetrahedral	4	[15]
Cp*BeCl	−14.88	C_6D_6	aromatic (η^5)	6	[10]
Cp*BeBr	−14.81	C_6D_6	aromatic (η^5)	6	[10]
Cp*BeI	−15.78	C_6D_6	aromatic (η^5)	6	[10]
DDPBeCl	12.2	C_6D_6	trigonal planar	3	[16,17]
DDPBeI	13.4	C_6D_6	trigonal planar	3	[16,17]
$Ph_2P(NDipp)_2BeCl$	11.36	C_6D_6	trigonal planar	3	[18]

Table 1. *Cont.*

Compound	^{9}Be NMR Shifts (δ in ppm)	Solvent	Coordination Mode	Coordination Number	Literature
$Ph_2P(NDipp)_2BeBr$	11.94	C_6D_6	trigonal planar	3	[18]
$Ph_2P(NDipp)_2BeI$	11.53	C_6D_6	trigonal planar	3	[18]
TerphenylBeCl·(Et_2O)	12.8	C_6D_6	trigonal planar	3	[13]
TerphenylBeBr·(Et_2O)	13.4	C_6D_6	trigonal planar	3	[13]
[1,3-($SiMe_3$)2C_3H_3]$_2$Be·(Et_2O)	18.2	C_6D_6	trigonal planar	3	[19]
Be[N($SiMe_3$)$_2$]$_2$	12.3	C_6D_6	linear	2	[4]
Be[N($SiMe_3$)$_2$]$_2$	9.6	thf-d_8	linear	2	[4]
Be[N($SiMe_3$)$_2$]$_2$	12.4	tol-d_8	linear	2	[4]

Cp = cyclopentadienyl (C_5H_5), Tp = 1-Tris(pyrazolyl)borate, Tp^{t}Bu = Tris(3-*tert*-butylpyrazolyl)hydroborato, Cp* = Pentamethylcyclopentadienyl (C_5Me_5), DDP = 2-((2,6-diisopropylphenyl)amino)-4-((2,6-diisopropylphenyl)imino)-pent-2-enyl), $Ph_2P(NDipp)_2$ = *N*,*N*′-bis(2,6-diisopropylphenyl) aminoiminodi(phenyl)phosphorane, Terphenyl = 2,6-di(2,4,6-trimethylphenyl)phenyl.

2.3. Solid State Structure

Compound **2a** crystallizes in the monoclinic space group $P2_1/n$ with the molecule placed on the special position. Be is coordinated by Cl, its symmetry equivalent, a thf molecule, and a hypersilyl ligand in a slightly distorted tetrahedral fashion (Figure 1). Crystallographic data of **2a** are given in Tables S1–S5.

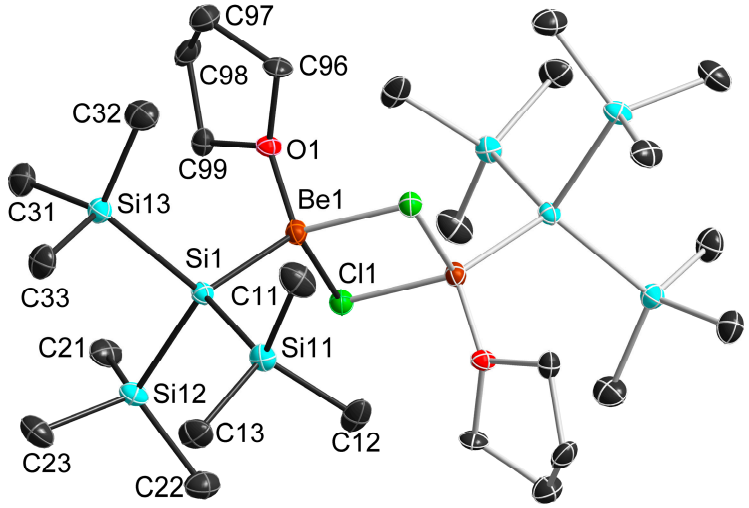

(**2a**)

Figure 1. Solid-state structures of **2a** (pale colored part generated by inversion); thermal ellipsoids are shown at 50% probability levels.

The bond angles around the central Be atom range from 96.5(2)° to 118.5(2)°, and the largest ones involve the central Si of the hypersilyl group. This distortion most likely results from the vast steric demand of the hypersilyl group. The Cl atom bridges the Be1 and its symmetry equivalent in a slightly asymmetric manner, as the difference between both Be–Cl bonds is about 0.1 Å. The Be–Cl bond lengths in **2a** (2.099(5), 2.112(5) Å) match well with the mean value of 2.02(7) Å for Be–Cl single bonds found in 48 structures with tetrahedrally coordinated Be atoms in the CSD [20]. The Be–O bond length also agrees with the mean value of 1.62(5) Å (187 hits), but weakly bonded thf molecules show Be–O bond lengths of up to 1.737 Å [21]. To the best of our knowledge, $CpBeSiMe_3$ [12] and Be(Si^{t}Bu$_3$)$_2$ [11] are the only compounds containing a Be–Si bond that to date have been structurally characterized. From these structure determinations, three independent values for the bond lengths are available (2.1930(10) Å, 2.2085(10) Å Be(Si^{t}Bu$_3$)$_2$ [22], and 2.185(2) Å $CpBeSiMe_3$ [12]). The fourth value available now from **2a** is in the same order but slightly larger (2:239(5) Å), which may again

be attributed to the high steric demand of the hypersilyl group. The Si–Si bond lengths and Si–Si–Si bond angles within the hypersilyl substituent are almost identical to those previously reported for compounds containing this specific substituent.

2.4. Quantum Chemical Calculations

Quantum chemical calculations were performed to gain a deeper understanding of the bonding situation in the heteroleptic complexes HypSiBeX·(thf) (HypSi = $Si(SiMe_3)_3$, X = F **1b**, Cl **2b**, Br **3b**, I **4b**). The crystal structure of **2a** was used as a starting point to model the gas phase structures of **1b**–**4b**. Geometries of these model structures were then optimized using RI-DFT [23–26] methods with the B3-LYP functional [27,28] and TZVPP basis sets [29] and third generation Becke–Johnson-damped dispersion correction [30,31]. To further investigate the influence of the coordination mode of Be on the NMR shift of this compound, additional model systems without the coordinated thf molecules were designed (**1c**–**4c**) and optimized with the same methods. NMR chemical shifts of **1b**–**4b** and **1c**–**4c** were calculated via GIAO methods [32]. Shared electron number (SEN) [33] calculations, electron localization function (ELF) [34,35] plots and localized orbital locator (LOL) [36] plots were performed for **1b**–**4b**.

The gas phase structures of **1b**–**4b** (Figure 2) are very similar to the crystal structure of **2a**. They each show dimeric structures, in which the Be atom adopts distorted tetrahedral coordination environments, and approximately show an inversion center between the two halide ligands (Figures S17–S20, Table S6). The two Be–X units approximately form a rhombus. Table 2 summarizes important bond lengths and angles of **2a** in comparison to those calculated for **1b**–**4b**.

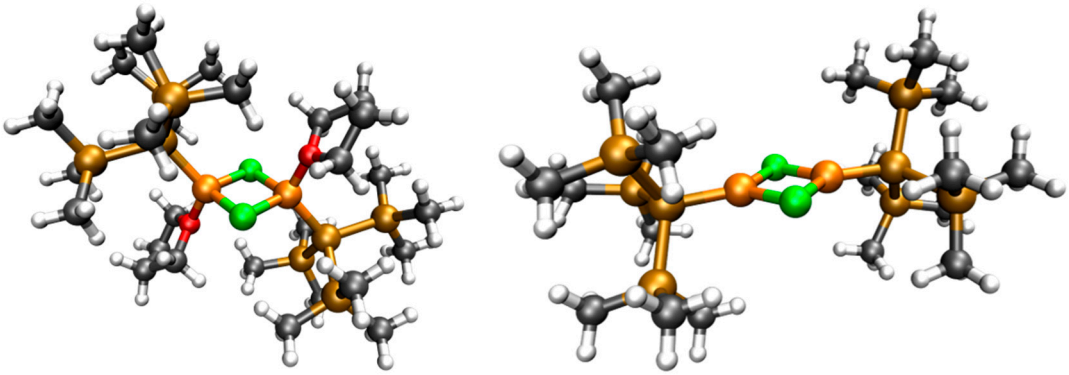

Figure 2. Calculated gas phase structure of **2b** (**left**) and **2c** (**right**); X displayed in green, Be in orange; Si in ocher, C in grey, O in red and H in white.

Table 2. Overview of calculated and observed bond lengths [Å] and angles [°] for **2a** and **1b**–**4b**.

	1b [1]	**2a**	**2b** [1]	**3b** [1]	**4b** [1]
Be–X	1.614	2.101 [1]	2.112	2.292	2.531
Be–Si	2.249	2.239(5)	2.222	2.213	2.203
Be–O	1.670	1.654(5)	1.670	1.655	1.649
X–Be–X	90.60	96.5(2)	97.4	98.2	99.0
Be–X–Be	89.4	83.5(2)	82.6	81.8	81.0
Si–Be–X_1	118.0	116.0(2)	114.6	113.6	112.0
Si–Be–X_2	123.5	118.5(2)	118.9	118.0	116.8
Si–Be–O	113.4	116.4(3)	115.7	117.1	118.5
Be–X–X–Be	180.0	180.0(3)	179.6	180.0	180.0
X–X–Be–Si	129.1	126.2(4)	136.7	125.5	123.8

[1] Values are averaged.

The Be–X bond lengths increase with increasing atomic number from F to I, while the Be–Si and Be–O bond lengths marginally decrease, which could be due to slightly reduced steric stress. In accord with Bent's rule and the steric demand of the halogen atoms, the X–Be–X angle increase with decreasing electronegativity and increasing atomic radii of the halide ion (X) from fluoride to iodide and the Be–X–Be angles consequently decrease. Moreover, the other angles also vary slightly. The crystal structure of **2a** is in good agreement with the calculated gas phase structure of **2b** for most displayed values. Slight differences in the Cl–Cl–Be–Si dihedral angle can be attributed to packing effects.

The gas phase structures of **1c**–**4c**, which have been calculated without any coordinating thf molecule, show trigonally coordinated Be atoms (Figures S21–S24). For **1c**–**3c**, the two Be–X units approximately lie in a rhombus (Be–X–X–Be dihedral angle of 179.7° to 178.5°), while that rhombus is significantly folded in **4c** (Be–X–X–Be dihedral angle of 163.6°). Similarly, Be and the halide substituents lie approximately in the same plane for **1c**–**3c** (X–X–Be–Si dihedral angle of 179.3° to 178.7°), while **4c** shows a significant deviation from planarity (X–X–Be–Si dihedral angle of 170.3°).

The calculated NMR chemical shifts (Table 3) of **1b**–**4b** and **1c**–**4c** are not very close to the measured signals, but fall in line with our calculations of other beryllium shifts, which tend to be higher than measured signals. Nonetheless, it can be clearly seen that there is a difference between the calculated chemical shifts of these substances for the thf-coordinated **1b**–**4b** in comparison to the thf-free **1c**–**4c**. Unfortunately, the shifts of these species overlap and one cannot clearly distinguish between thf-containing or thf-less species just by checking these theoretical values. Thus, a comparison with other measured Be-containing species is needed to evaluate or predict coordination modes.

Table 3. Overview of calculated and observed NMR shifts for **1**–**4**.

	1	**2**	**3**	**4**
a	–	2.45	–	−0.92
b	6.90	10.62	12.14	15.93
c	14.01	25.53	29.16	24.78

The Be–Si bonds were investigated by looking at their shared electron number (SEN) values. The values range from 1.42 for **1b** and 1.36 for **2b** and **3b**, to 1.31 for **4b**. These values are within the typical range for covalent bonds between Si–Si, Si–C and C–H in these molecules, which suggests that the Be–Si bond is quite covalent. This is exemplified further by looking at electron localization function (ELF) and localized orbital locator (LOL) plots (see also Figures S9–S16) of the Be–Si–Cl plane in Figure 3, where a Be–Si bond electron pair can clearly be seen around (*x*,*y*) = (6.58,4.52) bohr.

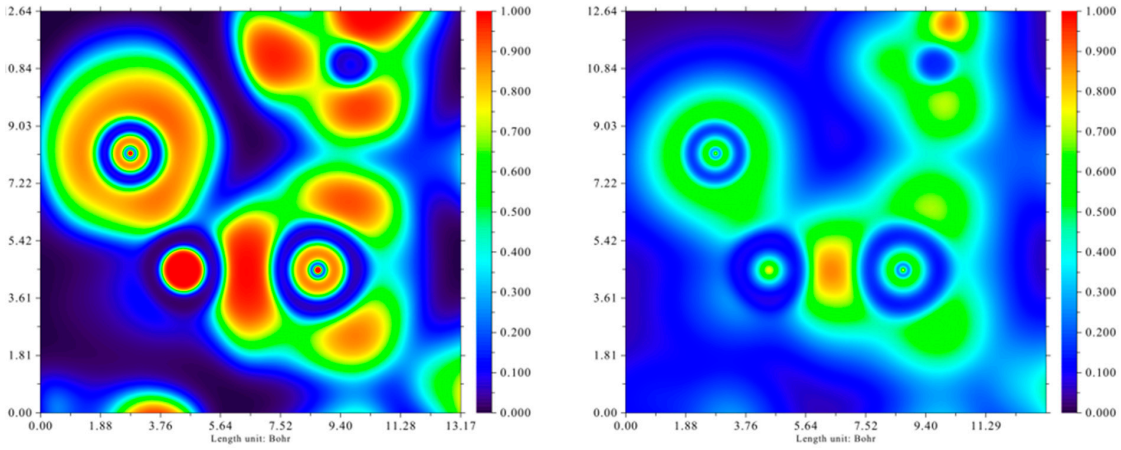

Figure 3. 2D-plots of the Si–Be–Cl plane: (**left**) ELF; (**right**) LOL.

3. Materials and Methods

Beryllium and its compounds are regarded as highly toxic and carcinogenic and they also have an allergic potential if inhaled with the risk of causing chronic beryllium disease (CBD) [37]. They should therefore be handled with appropriate safety precautions [8]. All experiments described herein were performed in fume hoods, in gloveboxes, or with advanced Schlenk techniques under extremely dry and oxygen-free (Caution) Ar atmosphere. HypSiLi·$(thf)_{2.6}$ was prepared in accordance with a procedure found in the literature [38]. The amount of coordinated thf in the HypSiLi·$(thf)_{2.6}$ was determined by adding a definite amount of 1,3,5-tri-^{t}Bu-benzene to the solution of the ligand in C_6D_6, followed by comparative integration of the signals. $BeCl_2$ and BeI_2 were synthesized from the elements at elevated temperatures followed by high-temperature, high-vacuum fractional sublimation [39]. NMR spectra were recorded on a Bruker Avance 300 spectrometer (Karlsruhe, Germany) at 25 °C at 300.1 MHz (^{1}H), 42.4 MHz (^{9}Be), 75.5 MHz (^{13}C), and 59.6 MHz (^{29}Si). ^{1}H and ^{13}C{^{1}H}–NMR spectra were referenced to internal C_6D_5H ($\delta(^1H)$ = 7.154 ppm; $\delta(^{13}C)$ = 128.0 ppm), ^{9}Be-NMR was referenced to external $BeSO_4$ in D_2O ($\delta(^9Be)$ = 0 ppm) and ^{29}Si spectra were referenced to an external standard of neat $Si(CH_3)_4$ ($\delta(^{29}Si)$ = 0 ppm). Elemental analyses were not determined because of the potential toxicity of the complexes. The purity of the compounds was verified by NMR spectroscopy. All reactions were performed under an argon atmosphere.

General Procedure for the Synthesis of HypSiBeX·(thf) (X = Cl ***2a****, I* ***4a****)*

Equimolar amounts of HypSiLi·$(thf)_{2.6}$ (0.221 g, 0.5 mmol) and BeX_2 (X = Cl 0.040 g, 0.5 mmol, I 0.131 g, 0.5 mmol) were dissolved in a mixture of toluene (20 mL) and thf (1 mL). The resulting solution was heated to 60 °C and stirred for 16 h. After that, all volatiles were removed in vacuum, and the residue was dried for an additional 2 h in an oil-pump vacuum. The residue was extracted with 2 mL of toluene and 1 mL of thf and filtrated by using a Teflon cannula, which was covered with a glass micro fiber filter (Whatman®, ME14 2LE Maidenstone, Kent, UK). Compounds **2a** and **4a** were obtained after storage of the clear solutions at −28 °C for 12 h.

HypSiBeCl·(thf) (**2a**): Yield: 140 mg (96%). ^{1}H NMR (300 MHz, thf-d_8, 25 °C): δ = 0.18 (s, 27H, Me), 1.72 (s (broad), 0.54H, thf), 3.58 (s (broad), 0.62H, thf). ^{9}Be NMR (C_6D_6, 42.2 MHz, 25 °C): δ = 2.45 (s). ^{13}C NMR (125 MHz, C_6D_6, 25 °C): δ = 1.68 (s, Me), 25.46 (thf), 67.58 (thf). ^{29}Si NMR (59.6 MHz, C_6D_6, 25 °C): δ = −82.05 (s, $(Me_3Si)_3Si$, −12.99 (s, $(Me_3\mathit{Si})_3Si$).

HypSiBeI·(thf) (**4a**): Yield: 157 mg (93%). ^{1}H NMR (300 MHz, thf-d_8, 25 °C): δ = 0.17 (s, 27H, Me), 1.74 (quint., 5.83H, thf), 3.58 (quint., 5.03H, thf). ^{9}Be NMR (C_6D_6, 42.2 MHz, 25 °C): δ = −0.92 (s). ^{13}C NMR (125 MHz, C_6D_6, 25 °C): δ = 1.87 (Me), 25.37 (thf), 67.46 (thf). ^{29}Si NMR (59.6 MHz, C_6D_6, 25 °C): δ = −83.94 (s, $(Me_3Si)_3\mathit{Si}$, −14.91 (s $(Me_3\mathit{Si})_3Si$).

Single crystal X-ray diffraction. [C_{26} H_{70} Be_2 Cl_2 O_2 Si_8], M = 728.46, colorless crystal (0.07 mm × 0.05 mm × 0.05 mm); monoclinic, space group $P2_1/n$; a = 10.3667(7) Å, b = 18.8628(12) Å, c = 11.3870(7) Å; α = 90°, β = 98.150(4)°, γ = 90°, V = 2204.2(2) Å^3; Z = 2; μ = 0.386 mm^{-1}; ϱ_{calc} = 1.098 g·cm^{-3}; 17848 reflections (θ_{max} = 26.46°), 4491 unique (R_{int} = 0.1159); 190 parameters; largest max./min in the final difference Fourier synthesis 0.451 e·Å^{-3}/−0.407 e·Å^{-3}; max./min. transmission 0.75/0.67; R_1 = 0.0564 ($I > 2\sigma(I)$), wR_2 = 0.1242 (all data).

The crystal was mounted on a nylon loop in inert oil. Data were collected on a Bruker AXS D8 Kappa diffractometer with APEX2 detector (mono-chromated Mo$K\alpha$ radiation, λ = 0.71073 Å). The structure was solved by Direct Methods (SHELXS-97) [40] and refined anisotropically by full-matrix least-squares on F^2 (SHELXL-2014) [41,42]. Absorption correction was performed semi-empirically from equivalent reflections on basis of multi-scans (Bruker AXS APEX2, Karlsruhe, Germany). Hydrogen atoms were refined using rigid methyl groups.

CCDC-1539267 contains the supplementary crystallographic data for this paper. These data can be obtained free of charge from The Cambridge Crystallographic Data Centre via www.ccdc.cam.ac.uk/data_request/cif.

4. Conclusions

We successfully synthesized compounds of the general type HypSiBeX·(thf) (HypSi = $Si(SiMe_3)_3$, X = Cl **2a**, I **4a**) bearing a Be–Si–bond and structurally characterized (**2a**), the third example of such a compound. The bond lengths in **2a** were compared with those obtained from quantum chemical calculations, which were expanded to the other halides as well as on the solvent-free complexes. Further analysis of the calculated data provided a deeper insight into so far not properly investigated Be–Si bond and demonstrated that the Be–Si–bond is mainly covalent (SEN: 1.4-1.3). The calculated ^{9}Be NMR shifts shows that tetrahedral coordination mode is also present in solution, which fits well to the reported ^{9}Be NMR shifts of comparable compounds.

Supplementary Materials: The following are available online at www.mdpi.com/2304-6740/5/2/22/s1, Figures S1–S24, Tables S1–S6, cif and checkcif files.

Acknowledgments: Stephan Schulz thanks the University of Duisburg-Essen for financial support and Dieter Bläser for collecting the crystallographic data.

Author Contributions: Dominik Naglav, Kevin Dzialkowski, and Stephan Schulz conceived and designed the experiments; Dominik Naglav and Kevin Dzialkowski performed the experiments; Christoph Wölper analyzed the X-ray structure; Briac Tobey and Georg Jansen performed and analyzed the quantum mechanical calculations; Dominik Naglav and Kevin Dzialkowski analyzed the NMR data; Dominik Naglav, Briac Tobey, Kevin Dzialkowski, Christoph Wölper, and Stephan Schulz wrote the paper.

Conflicts of Interest: The authors declare no conflict of interest.

References

1. Iversen, K.J.; Couchman, S.A.; Wilson, D.J.; Dutton, J.L. Modern organometallic and coordination chemistry of beryllium. *Coord. Chem. Rev.* **2015**, *297–298*, 40–48. [CrossRef]
2. Arrowsmith, M.; Braunschweig, H.; Celik, M.A.; Dellermann, T.; Dewhurst, R.D.; Ewing, W.C.; Hammond, K.; Kramer, T.; Krummenacher, I.; Mies, J.; et al. Neutral zero-valent s-block complexes with strong multiple bonding. *Nat. Chem.* **2016**, *8*, 638–642. [CrossRef] [PubMed]
3. Arrowsmith, M.; Hill, M.S.; Kociok-Kohn, G.; MacDougall, D.J.; Mahon, M.F. Beryllium-induced C–N bond activation and ring opening of an *N*-heterocyclic carbene. *Angew. Chem. Int. Ed. Engl.* **2012**, *51*, 2098–2100. [CrossRef] [PubMed]
4. Naglav, D.; Neumann, A.; Bläser, D.; Wölper, C.; Haack, R.; Jansen, G.; Schulz, S. Bonding situation in $Be(N(SiMe_3)_2)_2$—An experimental and computational study. *Chem. Commun.* **2015**, *51*, 3889–3891. [CrossRef] [PubMed]
5. Bayram, M.; Naglav, D.; Wölper, C.; Schulz, S. Synthesis and Structure of Bis(diphenylphosphinimino)methanide and Bis(diphenylphosphinimino)methanediide Beryllium Complexes. *Organometallics* **2016**, *35*, 2378–2383. [CrossRef]
6. Buchner, M.R.; Müller, M.; Rudel, S.S. Beryllium Phosphine Complexes: Synthesis, Properties, and Reactivity of $(PMe_3)_2BeCl_2$ and $(Ph_2PC_3H_6PPh_2)BeCl_2$. *Angew. Chem. Int. Ed. Engl.* **2017**, *56*, 1130–1134. [CrossRef] [PubMed]
7. Zhu, H.; Li, Y.; Zhu, G.; Su, H.; Chan, S.H.; Sun, Q. $Be_{12}O_{12}$ Nano-cage as a Promising Catalyst for CO_2 Hydrogenation. *Sci. Rep.* **2017**, *7*, 40562. [CrossRef] [PubMed]
8. Naglav, D.; Buchner, M.R.; Bendt, G.; Kraus, F.; Schulz, S. Off the Beaten Track—A Hitchhiker's Guide to Beryllium Chemistry. *Angew. Chem. Int. Ed. Engl.* **2016**, *55*, 10562–10576. [CrossRef] [PubMed]
9. Naglav, D.; Bläser, D.; Wölper, C.; Schulz, S. Synthesis and characterization of heteroleptic 1-tris(pyrazolyl)borate beryllium complexes. *Inorg. Chem.* **2014**, *53*, 1241–1249. [CrossRef] [PubMed]
10. Naglav, D.; Tobey, B.; Neumann, A.; Bläser, D.; Wölper, C.; Schulz, S. Synthesis, Solid-State Structures, and Computational Studies of Half-Sandwich Cp*BeX (X = Cl, Br, I) Compounds. *Organometallics* **2015**, *34*, 3072–3078. [CrossRef]
11. Lerner, H.-W.; Scholz, S.; Bolte, M.; Wiberg, N.; Nöth, H.; Krossing, I. Synthesis and Structures of Alkaline-Earth Metal Supersilanides: $^tBu_3SiMX$ and $^tBu_3Si{-}M{-}Si^tBu_3$ (M = Be, Mg; X = Cl, Br). *Eur. J. Inorg. Chem.* **2003**, *2003*, 666–670. [CrossRef]

12. Saulys, D.A.; Powell, D.R. Synthesis, Experimental/Theoretical Characterization, and Thermolysis Chemistry of CpBe($SiMe_3$), a Molecule Containing an Unprecedented Beryllium–Silicon Bond. *Organometallics* **2003**, *22*, 407–413. [CrossRef]
13. Niemeyer, M.; Power, P.P. Synthesis, ^{9}Be NMR Spectroscopy, and Structural Characterization of Sterically Encumbered Beryllium Compounds. *Inorg. Chem.* **1997**, *36*, 4688–4696. [CrossRef] [PubMed]
14. Ruhlandt-Senge, K.; Bartlett, R.A.; Olmstead, M.M.; Power, P.P. Synthesis and Structural Characterization of the Beryllium Compounds [Be(2,4,6-$Me_3C_6H_2)_2(OEt_2)$], [Be{O(2,4,6-*t*-$Bu_3C_6H_2$}(OEt_2)], and [Be{S(S(2,4,6-*t*-$Be_3C_6H_2$)}$_2$(thf)]$_2$(THF)]PhMe and Determination of the Structure of [$BeCl_2(OEt_2)_2$]. *Inorg. Chem.* **1993**, *32*, 1724–1728. [CrossRef]
15. Han, R.; Parkin, G. [Tris(3-tert-butylpyrazolyl)hydroborato]beryllium hydride: Synthesis, structure, and reactivity of a terminal beryllium hydride complex. *Inorg. Chem.* **1992**, *31*, 983–988. [CrossRef]
16. Arrowsmith, M.; Hill, M.S.; Kociok-Kohn, G.; MacDougall, D.J.; Mahon, M.F.; Mallov, I. Three-coordinate beryllium beta-diketiminates: Synthesis and reduction chemistry. *Inorg. Chem.* **2012**, *51*, 13408–13418. [CrossRef] [PubMed]
17. Arrowsmith, M.; Crimmin, M.R.; Hill, M.S.; Kociok-Kohn, G. Beryllium derivatives of a phenyl-substituted beta-diketiminate: A well-defined ring opening reaction of tetrahydrofuran. *Dalton Trans.* **2013**, *42*, 9720–9726. [CrossRef] [PubMed]
18. Naglav, D.; Tobey, B.; Dzialkowski, K.; Jansen, G.; Neumann, A.; Bläser, D.; Wölper, C.; Schulz, S. Synthesis and Characterization of Heteroleptic Diiminophosphinate Beryllium Complexes. Unpublished results. 2017.
19. Chmely, S.C.; Hanusa, T.P.; Brennessel, W.W. Bis(1,3-trimethylsilylallyl)beryllium. *Angew. Chem. Int. Ed. Engl.* **2010**, *49*, 5870–5874. [CrossRef] [PubMed]
20. Allen, F.H. The Cambridge Structural Database: A quarter of a million crystal structures and rising. *Acta Crystallogr. Sect. A Found. Crystallogr.* **2002**, *58*, 380–388. [CrossRef]
21. Lorenz, V.; Fischer, A.; Edelmann, F.T. Silsesquioxane chemistry, The first beryllium silsesquioxane: Synthesis and structure of [$Cy_7Si_7O_{12}BeLi]_2$ 2THF. *Inorg. Chem. Commun.* **2000**, *3*, 292–295. [CrossRef]
22. Lerner, W.; Goethe-Universität Frankfurt, Frankfurt, Germany. Supply of the value for the second independent molecule. Personal Communication, 2017.
23. Treutler, O.; Ahlrichs, R. Efficient molecular numerical integration schemes. *J. Chem. Phys.* **1995**, *102*, 346–354. [CrossRef]
24. Eichkorn, K.; Treutler, O.; Öhm, H.; Häser, M.; Ahlrichs, R. Auxiliary basis sets to approximate Coulomb potentials. *Chem. Phys. Lett.* **1995**, *240*, 283–290. [CrossRef]
25. Eichkorn, K.; Weigend, F.; Treutler, O.; Ahlrichs, R. Auxiliary basis sets for main row atoms and transition metals and their use to approximate Coulomb potentials. *Theor. Chim. Acta* **1997**, *97*, 119–124. [CrossRef]
26. Von Arnim, M.; Ahlrichs, R. Performance of parallel TURBOMOLE for density functional calculations. *J. Comput. Chem.* **1998**, *19*, 1746–1757. [CrossRef]
27. Becke, A.D. Density-functional thermochemistry. III. The role of exact exchange. *J. Chem. Phys.* **1993**, *98*, 5648–5652. [CrossRef]
28. Stephens, P.J.; Chabalowski, C.F.; Frisch, M.J. Ab Initio Calculation of Vibrational Absorption and Circular Dichroism Spectra Using Density Functional Force Fields. *J. Chem. Phys. Chem.* **1994**, *98*, 11623–11627. [CrossRef]
29. Weigend, F.; Ahlrichs, R. Balanced basis sets of split valence, triple zeta valence and quadruple zeta valence quality for H to Rn: Design and assessment of accuracy. *Phys. Chem. Chem. Phys. PCCP* **2005**, *7*, 3297–3305. [CrossRef] [PubMed]
30. Grimme, S.; Antony, J.; Ehrlich, S.; Krieg, H. A consistent and accurate ab initio parametrization of density functional dispersion correction (DFT-D) for the 94 elements H–Pu. *J. Chem. Phys.* **2010**, *132*, 154104. [CrossRef] [PubMed]
31. Grimme, S.; Ehrlich, S.; Goerigk, L. Effect of the damping function in dispersion corrected density functional theory. *J. Comput. Chem.* **2011**, *32*, 1456–1465. [CrossRef] [PubMed]
32. Kollwitz, M.; Gauss, J. A direct implementation of the GIAO-MBPT(2) method for calculating NMR chemical shifts. Application to the naphthalenium and anthracenium ions. *Chem. Phys. Lett.* **1996**, *260*, 639–646. [CrossRef]
33. Davidson, E.R. Electronic Population Analysis of Molecular Wavefunctions. *J. Chem. Phys.* **1967**, *46*, 3320–3324. [CrossRef]

34. Becke, A.D.; Edgecombe, K.E. A simple measure of electron localization in atomic and molecular systems. *J. Chem. Phys.* **1990**, *92*, 5397–5403. [CrossRef]
35. Silvi, B.; Savin, A. Classifaction of chemical bonds based on topological analysis of electron localization functions. *Nature* **1994**, *371*, 683–686. [CrossRef]
36. Schmider, H.; Becke, A. Chemical content of the kinetic energy density. *J. Mol. Struct. THEOCHEM* **2000**, *527*, 51–61. [CrossRef]
37. Kumberger, O.; Schmidbaur, H. Warum ist Beryllium so toxisch? *Chem. Unserer Zeit* **1993**, *27*, 310–316. [CrossRef]
38. Gutekunst, G.; Brook, A.G. Tris(trimethylsilyl)silyllithium·3 thf: A stable crystalline silyllithium reagent. *J. Organomet. Chem.* **1982**, *225*, 1–3. [CrossRef]
39. Brauer, G. *Handbuch der Präparativen Anorganischen Chemie*, 3rd ed.; Ferdinand Enke: Stuttgart, Germany, 1975; Volume 1.
40. Sheldrick, G.M. Phase annealing in *SHELX*-90: Direct methods for larger structures. *Acta Crystallogr. A Found. Crystallogr.* **1990**, *46*, 467–473. [CrossRef]
41. Sheldrick, G.M. A short history of *SHELX*. *Acta Crystallogr. Sect A Found. Crystallogr.* **2008**, *64*, 112–122. [CrossRef] [PubMed]
42. Hubschle, C.B.; Sheldrick, G.M.; Dittrich, B. *ShelXle*: A Qt graphical user interface for *SHELXL*. *J. Appl. Crystallogr.* **2011**, *44*, 1281–1284. [CrossRef] [PubMed]